Mapping spatial distribution of soil properties using electrical resistivity on a long term sugarcane trial in South Africa

Gaghik Hovhannissian, Pascal Podwojewski, Yann Le Troquer, Sandile Mthimkhulu, Rianto van Antwerpen

Mapping spatial distribution of soil properties using electrical resistivity on a long term sugarcane trial in South Africa

Gaghik Hovhannissian[1], Pascal Podwojewski[1] Yann Le Troquer[1], Sandile Mthimkhulu[2], Rianto Van Antwerpen[2,3]

[1] IRD, UMR IEES-Paris, SU/IRD/CNRS/INRA/UPEC/Univ. Paris Diderot, Centre IRD de France Nord, 32, Av. H. Varagnat, 93143 Bondy cedex. France

[2]South African Sugar Association Experiment Station, Private Bag X02, Mount Edgecombe, 4300, South Africa

[3]Department of Soil, Crops and Climate Sciences, University of the Free State, PO Box 339, Bloemfontein 9300, South Africa

Abstract

In experimental trials the spatial distribution of soil properties is a key factor to evaluate and determine the credibility of the research outcomes. To evaluate the spatial distribution of soil properties at different depths in the present study, the electrical resistivity method was selected because of its non-destructive nature and high spatial resolution.

The investigation was conducted on BT1 (Burning versus mulching) the world's oldest sugarcane trial (established 25 October 1939) located on the premises of the South African Sugarcane Research Institute (SASRI). The experimental area, covering 7200 m^2, is divided in 32 plots with three crop residue retention treatments. These treatments are either fertilized and not fertilized. The RM15 resistance-meter equipped with a multiplexer was used to collect geophysical data. The latter was used to generate apparent electrical resistivity maps corresponding to three approximate depth ranges: (0 - 0.5 m, 0 - 1.0 m and 0 – 2.0 m). The spatial resolution of the shallowest map (0 - 0.5 m), was 0.5 m x 1.0 m. Bulk density and soil water content, for the 0 - 0.1 m depths, were also determined from samples collected on a grid of 4 m x 5 m. All data collected were georeferenced using a spatial resolution of 4 m x 1 m with the Digital Elevation Model (DEM).

The results of this survey showed the effectiveness of geophysical mapping to reveal detailed information regarding soil spatial variability and to understand and establish the relationships between soil fertility and soil physical properties. Detailed analysis of these results led to the identification of two different soil types on the trial site: a Mollic Cambisol in the upper slope of the trial with a depth of less than 1.0 m and a deeper Mollic Nitisol in the lower slope. Additionally, close to the southern edge of the site, higher values of electrical resistivity revealed a layer of colluvial deposits, that has not been considered in the past. The relationships between electrical resistivity and investigated soil properties (soil water content, bulk density, aggregate stability and fertilizer) initially seemed paradoxical. Although there is still a need for further investigations, the current study decently establish the rather unexpected relationships. The most striking finding was the high resistivity in fertilised plots associated with the application of potassium chloride fertiliser which led to a decreased soil aggregate stability.

Key words: electrical resistivity mapping, sugarcane, mulch, fertilizer, bulk density, soil water content, soil physical properties, long term trial.

1. Introduction

The current study was conducted in the long-term continuously monitored sugarcane trial (BT1). This trial commenced in October 25, 1939 at the South African Sugarcane Research Institute (SASRI) located in Mount Edgecombe (near Durban) to investigate the effect of greencane harvesting and burning of sugarcane prior to harvest as well as continuous fertiliser application on soil and cane yields (Van Antwerpen et al., 2001). There are several studies that have been conducted in this trial to monitor the changes in soil and crop yield (Van Antwerpen et al., 2001; Graham et al., 2002; Mthimkhulu et al., 2016)..

These studies have revealed that burning of sugarcane prior to harvest under the monocultural system and conventional tillage leads to a decline in soil carbon content (SOC) and soil fertility. Their findings also showed that greencane harvesting, an alternative to pre-harvest burning, encourages the retention and mulching of all leafy non-sucrose containing crop material on the soil surface and potentially increase SOC (Graham et al., 2002). The most recent investigation by Mthimkhulu et al. (2016) reported a significant increase in acidity and a decrease in soil aggregate stability and base cations (calcium and magnesium) which was attributed to mining of nutrients by sugarcane, nitrification and subsequent leaching of base cations. However, none of these studies conducted a precise soil mapping of the trial to provide systematic georeferenced information on the spatial distribution of soil physical characteristics such as depth, texture, bulk density, aggregate stability and soil water properties that might be influenced by the treatments and topography.

Topography is generally one of the major factors in soil formation and its impact is very important on agricultural fields in terms of soil spatial variability, nutrients concentration and leaching of chemicals (mineral fertilizers) and, therefore, has a significant influence on the crop yields (Biggar and Nielsen, 1976; Yang et al., 1998; Iqbal et al., 2005; Senthilkumar et al., 2009). Terrain relative elevation, shape of the relief, slope gradient, as well as its orientation and its amplitude represent important topographical factors of the soil evolution. They define the principal properties of hydrological functioning of the arable land, like the water flux potential and the peculiarities of the runoff erosion, or sediments transport and deposition (Moore and Burch, 1986; Changere and Lal, 1997; Bakhsh et al., 2000; Kravchenko and Bullock, 2002). Under certain conditions, these phenomena are considered as the main cause of the decline in soil quality on a cultivated steep hillslope (Li and Lindstrom, 2001).

Generally the annual input of organic matter is expected to have a considerable effect on soil porosity, soil structure (Blair, 2000) and soil water content as mentioned by Robertson (2003) but data are scarce. The stability of the aggregates and the connectivity of pores between them is well known to affect the movement and storage of water, aeration, erosion, biological activity and the growth of crops (Amezketa, 1999, Boix-Fayos et al., 2001).

In order to better our understanding of these soil properties and their response to external factors such as topography and land management practices precise mapping is required. Classical approach to mapping soil physical properties is based on data collected at discrete observation points; detailed mapping thus becomes very costly when a large number of data points are required. Opening soil profile pits and sampling large volumes of soil are generally requested for that purpose. However, this *modus operandi* can be very destructive and impossible in an experimental trial covering a relatively small area, and where intensive soil disturbance is unwanted. In this context, the use of geophysical methods has been proven to be efficient and meaningful in the non-intrusive collection of data (Corwin and Lesch, 2003; Samouëlian et al., 2005). As demonstrated in several studies, geophysical techniques, such as electrical resistivity mapping, are very well adapted for use on agronomic trial sites (Corwin and Lesch, 2005; Tabbagh et al., 2000). However an empirical relationship needs to be established for each site between soil electrical resistivity values and soil physical properties as these relationships may be site-specific (Friedman, 2005). Examples of such relationships have been published for water content and bulk density (Cousin et al., 2005), waterlogged soil horizons and spatial-temporal distribution of soil water following irrigation (Michot et al., 2003; McCucheon et al., 2006). Geophysical methods have also been used to study soil textural changes with depth, to evaluate soil thickness *i.e.* the depth to the parent rocks (Milsom, 2003), to locate the presence and to define the thickness of compacted or low density horizons, and to characterise textural properties in duplex soils (McCarter, 1984). It has also been found very efficient in assessing soil salinity through increased electrical conductivity values (Rhoades et al. 1989).

To characterize the spatial distribution of the different soil properties in the BT1 experimental site, we applied the method of electrical resistivity mapping with high spatial resolution, corresponding to 3 different depths of investigation.

The main objectives of this study were: i.) to collect information on soil spatial variability, soil thickness and pedological changes within the trial, down to approximately 2 m depth; ii.) to analyse and identify changes in electrical resistivity related to soil characteristics, such as water content or bulk density; and, iii.) to assess the impact of different treatments (mulch, fertilization, etc.) on the evolution of soil properties in the experimental plots.

2. Material and methods

2.1 Site location, soil properties

The experimental site (BT1) is located on the premises of the South African Sugarcane Research Institute, at Mount Edgecombe, in KwaZulu-Natal province, South Africa (31°02'41.10" E ; 29°42'10.82" S). The highest elevation which corresponds to the North-Eastern corner is 99 m above sea level (a.s.l.), with an average slope of 15% facing South-West (Fig.1a). The surface of this experimental site has a parallelogram shape, nearly rectangular, and covers an area of 7200 m² (90 m x 80 m) with the following corner coordinates (36J 310840 E, 6712525 N; 36J310805 E, 6712455 N; 36J310730 E, 6712490 N; 36J310765 E, 6712560 N) in the Universal Transverse Mercator (UTM) geographic coordinates system (Fig.1b).

The regional climate is subtropical humid and is characterized by summer (October–March) rainfall. The average annual precipitation is 950 mm, and the average annual temperature is 20.4°C.

The soil was initially classified as Vertisol, (Graham et al. 2002) with a dark (2.5YR 3/1 to 3/2) 50 cm thick **A** horizon extending to a dark reddish brown (2.5YR 3/3 to 3/4) AC transitional horizon overlying weathered dolerite. The profile in the upper slope contained a 5 cm thick stone-line at a depth of about 30-40 cm overlying weathered dolerite (Fig.2). On the lower slope, the soil has the same A horizon as the upper slope, but overlying a red (2.5YR 3/4 to 10R 3/6) B horizon. The soil texture of the **A** horizon is generally clayey with a little over 40 % of clay and less than 20% of sand in the upper 20 cm. Downstream, in the lower part of the slope, the soil texture becomes clay - loamy with the sand content slightly above 20%. The clay mineralogy is dominated by kaolinite with some scattered evidences of smectite. The soil pH in water is ranging between 4.2 and 5.7. More details of the trial and analytical methods are described by Mthimkhulu et al. (2016).

2.2 Experimental design

This experimental site has been described in details by Thompson (1966), Van Antwerpen and Meyer (1998), and Van Antwerpen et al., (2001). The complete trial is composed of 32 plots divided in 4 columns and 8 rows (Fig.1b). Each plot of 175 m^2 is 18 m long and 9.6 m wide. In each plot the sugarcane is planted in 7 rows parallel to the plot long edge and spaced 1.37 m. The treatments were: 1) Unburned at harvest with the residue (mainly brown and green leaves) retained on the soil surface to provide a mulch cover (M); 2) Sugarcane burned at harvest with the partially unburned green tops scattered evenly over the soil surface (BS);

3) Sugarcane burned at harvest with the unburned green tops removed from the soil surface (BR). These treatments were further subdivided into fertilized (F) and unfertilized plots (F0) in a split-plot design with eight replications for M and four replications for BS and BR treatments.

Since the trials' inception in October 25, 1939, the soil at the site has been disturbed only seven times. Initially replanting involved conventional tillage, which imply that the total trial area was ploughed in preparation for planting. In 1970, minimum tillage was adopted with disturbance of the planting row only. All fertilized treatments received 140 kg of nitrogen (N) (as $(NH)_2$ SO_4 - ammonium sulphate), 28 kg of phosphorus (P) (as P_2O_5 - superphosphate) and 140kg of K (as KCl – potassium chloride) per hectare, applied as 5:1:5 (46%) at 670 kg ha^{-1} approximately 40 days after harvesting (van Antwerpen et al., 2001). There were small fluctuations of the fertilizer composition during the last 20 years. No compensation is made for the nutrients recycled through the retention of residue after harvest. Since 1987 the crop is annually harvested in spring (September) at the beginning of the rainy season.

It may be added that the presence of termite nests of *Odontotermes sp.* was evidenced by vertical chimneys deeper than 0.6 m and with a diameter of 0.15 m at the north of plot 9 and west of plot 22 (Fig. 1b). In that area, termite nests are generally located on the external border of sugarcane plot surrounded by grass pathways.

2.3 Topographic survey

A high precision topographic map of the study area was created using a laser tacheometer (LEICA Total Station - TC 302). The use of this equipment made it possible to determine the horizontal coordinates (X and Y) with errors less than ± 0.10 m, and the altitude Z, with errors smaller than ± 0.05 m.

This survey was carried out for two reasons: (i) in order to be able to study the impact of topography on soil properties at large; (ii) and to define the georeferenced coordinates of each plot and their boundaries with high precision. For the elevation model, the measurements over the entire site were made at the nodes of a 4 m x 1 m rectangular grid. A 0.5 m mesh digital elevation model (DEM) was generated using these results, which provides the accuracy and density of measurement points required. Thanks to this model, all actions and experimental interventions (positions of different sensors, auger soundings or pedological pits, etc.) could be now georeferenced.

2.4 Soil water content and bulk density

The soil samples used for the determination of soil water content (SW) and bulk density (BD) were collected from the whole trial area at the 0–10 cm soil layer, following a 4 m x 5 m grid. This sampling was made simultaneously with measurements of electrical resistivity. A total of 325 undisturbed soil cores (250 cm^3) were collected: 275 within the plots and 50 within the alleys. All the samples were oven dried at 105°C for 24 hours. The final results will be presented as two maps (SW and BR) where the "Nearest Neighbour" data interpolation method has been used for both parameters.

2.5 Soil structural stability

The soil structural stability was determined on the soil samples using the fast wetting AFNOR (2005) method developed by Le Bissonais (1996). The aggregate stability data, calculated from a nest of six sieves (2, 1, 0.5, 0.2, 0.1 and 0.05 mm), was converted to mean weight diameter (MWD) according to Kemper and Rosenau (1986). Three replicate soil samples used to measure this parameter were collected at two depths (0-10 and 10-20 cm, i.e. six samples per plot) from three mini-pits in each of the thirty-two plots. The total of samples analysed for MWD was 192.

2.6 Apparent electrical resistivity mapping

Electrical resistivity mapping of the whole trial, including breaks between plots, was carried out in November 2011, after harvesting that took place in September, but prior to the annual fertilization.

For the measurements we used the so called "pole-pole" configuration of electrodes, consisting of two mobile electrodes (the current electrode and the potential electrode) with the second pair (current and potential) of electrodes remote and fixed far enough from the prospecting area, to be considered as an infinite distance. This condition is satisfied if the remote electrodes are placed at a distance greater than 20 times the spacing between the mobile electrodes (Robain et al., 1999). The use of the "pole-pole" electrode array is justified because it reduces the number of mobile electrodes from 4 to 2 for each measurement, and thus allow high productivity. This electrode configuration is relatively sensitive to non-horizontal boundaries and heterogeneities and provides greater depths of investigation, compared to other arrays (Seaton and Burbey, 2002). At the surface of a homogeneous medium, it measures the so-called “true resistivity” of the medium (ρ) (expressed in Ohm·m or Ω·m). It integrates a volume of medium roughly hemispheric around the 2 mobile electrodes, *i.e.* down to a depth roughly equal to the electrode spacing (Oldenburg and Li, 1999). At the surface of a non-homogeneous environment, in the case of our survey for instance, the equipotential surfaces around the current electrode are no more hemispheric; their actual geometry depends on the different media around the electrodes; it measures a so-called “apparent resistivity” (ρ_a) (expressed also in Ohm·m or Ω·m), related to the true resistivities of the surrounding media. Practical experience and numerical modelling however have proven that: (i) the greater the separation between the two electrodes, the greater the depth of exploration and (ii) apparent resistivity maps can be interpreted qualitatively and provide very useful information on the study site. Inversion procedures to transform apparent resistivities into 2 or 3 dimensional models with “true resistivities”, so-called “electrical tomographies”, require much heavier and costly field operations, which are performed only when detailed investigations and modelling are mandatory.

The measurements were performed using a "Resistance Meter RM-15" equipped with a "MPX15 multiplexer" and connected to a "PA20 multi-probe array" (Geoscan Research, Heather Brae, Chrisharben Park, Clayton, Bradford, West YorkshireBD14 6AE, UK).

To simplify the transportability of the instrument by a single operator from one point of measurement to the next, the resistance-meter and the multiplexer are fixed on a versatile frame whose basis is a beam with a length of 2 m, on which 5 stainless steel electrodes are mounted with a spacing **a** = 0.5 m. During mapping, the measurements were carried out moving the device forward with 1 m intervals along lines perpendicular to the northern edge, and with 2 m spacing between successive lines. Seven readings were recorded at each position of the device: 4 measurements with an electrode spacing of 0.5 m (**a** = 0.5 m); two measurements with electrode spacing of 1.0 m (**a** = 1.0 m) and one measurement with electrode spacing of 2.0 m (**a** = 2.0 m). The number of measurements obtained with a 0.5 m x 1.0 m 1.0 m x1.0 m, and 2.0 m x 1.0 m grid spacing were 13600; 6800 and 3400 data points respectively. We were thus able to draw and present three “apparent resistivity” maps representative of three soil thicknesses, approximately 0 - 0.5 m, 0 – 1 m and 0 – 2 m.

These maps were analysed by comparison with the topographic features, water content, bulk density, and aggregate stability characteristics, at the relevant depths (0 – 10 cm and 10 – 20 cm).

3. Results

3.1 Topographic survey

From our topographic survey, as mentioned above (§2.3), a 0.5 m mesh Digital Elevation Model (DEM) was generated. This model was used to determine slope gradients and other specific relief features were determined, as shown on Fig. 3. The highest absolute elevation was equal to 99 m a.s.l., while the lowest was 85 m a.s.l., isohypses every 0.5 m altitude difference, magnitude and azimuth of slope gradients as shown by vectors.

The surface of the trial is mainly facing southwest with the axis of the general slope coinciding approximately with the NE-SW diagonal. The average slope along this axis is 12 %, but it is not constant. It represents a convex then concave shape, with an average slope of 10-12 % close to the upper northeast corner; in the central part of the trial, the slope increases to 15-17 %, and then declines to 4-8 % at about 15-20 meters, near the southwest corner. The difference in altitude is larger at the eastern (10.5m) and northern edges (9.2 m), compared to the western (4.6 m) and southern edges (3.2 m). In addition, these slopes are neither uniform nor linear. So, it should however be noted that the topographic surface of the trial is rather complex and this can have major impacts on the soil properties.

On the map (Fig.3), the arrows indicate the energy and direction of the rainwater flows. They exhibit rather large differences in magnitude and azimuths: the flow direction is a) approximately perpendicular to the sugarcane rows in the eastern part of the site, b), it crosses the rows with an angle close to 45° in the central and south-western parts, and c) it is practically parallel to the rows in the north-western part. These important differences in intensity and direction of the water flows are major features of the trial site because of their substantial influence on the erosion and dissolution phenomena, as well as on the transport and deposition of solutes and suspended particles.

3.2 Soil water content and bulk density

The main SW results are shown on Fig. 4a and 4b. The points in Fig.4a indicate the positions where soil samples used for SW and the BD (bulk density) values were collected. The map of SW determined at 0-10 cm, indicated that this property is affected by crop residues retention treatment (i.e. M treatments show high values of SW).

The SW increased with increase in crop residues on the soil surface in fertilized and unfertilized treatments as anticipated (0.36 $kg \cdot kg^{-1}$ for (MF) plots >BSF (0.24 $kg \cdot kg^{-1}$) > BRF (0.19 $kg \cdot kg^{-1}$) and MF0 (0.32 $kg \cdot kg^{-1}$) > BSF0 (0.25 $kg \cdot kg^{-1}$ > BRF0 (0.20 $kg \cdot kg^{-1}$) (Fig. 4b).

The SW median values in MF treatment (0.36 kg·kg^{-1}) are slightly higher compared to the MF0 treatment (0.32 kg·kg^{-1}), and this could be attributed to the larger amount of residue material resulting from the combination of fertilizer and crop residues. The SW differences are observed between the fertilized and unfertilized plots were not significant for BS and BR treatments. Concerning the dispersion, *i.e.* the distance between the two extreme quartiles, it is rather small for BR and BS and greater at the M treatment.

Similarly to the SW map, with the soil bulk density (BD) map, all the M treatments were easy to identify (Fig.5a), The highest and the lowest bulk densities were measured at BR (1.18 g·cm^{-3}) and M treatments (0.82 g·cm^{-3}) respectively. The same statistical approach as above has been applied to each six populations (Fig.5b). The general trend showed a decrease in BD from 1.13 g·cm^{-3} at BRF0 to 1.0 g·cm^{-3} at the MF. Fertilized plots had lower BD values across all the crop residue treatments compared to F0. Besides the measurements are characterized by relatively high interquartile dispersions, indicating large heterogeneities in the density the investigated soil.

3.3 Soil structural stability (MWD)

The MWD are presented in Fig.6a and 6b, These results indicated that the MWD does not vary much relative to the residue treatments, but it decreased significantly in the F plots in both mulched and burnt treatments. The MWD in F0 ranged from 1.72 mm (BSF0) to 2.33 mm (BRF0) at 0 – 10 cm depths, and from 2.22 mm (MF0) to 2.41 mm (BRF0) at 10 – 20 cm depths.

It was also worth noting that MWD were slightly higher at 10 – 20 cm depths of F treatment, the median values ranging from 1.50 mm for MF to 1.75 mm for BRF, and from 1.11 mm for BRF to 1.37 mm for MF. at 0 – 10 cm depths. An increase in MWD (from 1.11 in BRF to 1.37 mm in MF) attributed to increase in crop residues was only observed at 0 – 10 cm of the F treatment. At 10 – 20 cm depths, it decreased, from 1.75 mm to 1.50 mm.

The results also show that the fertilizer application leads to a nearly identical light decrease in MWD values, from 0.6 mm to 0.8 mm, for all types of treatments at both depths, except for the difference between (BRF0) and (BRF) at 0 – 10 cm depths, where it is quite large (1.22mm), representing a variation greater than 50%.

3.4 Soil electrical resistivity mapping

Three apparent electrical resistivity (ρ_a) maps are shown on Fig.7 a, b and c, corresponding to three increasing thicknesses, as explained above, since they represent the results of measurements with increasing electrode spacing **a**, from 0.5 m to 1.0 m and to 2.0 m.

The map representing the measurements with electrode spacing **a** = 0.5 m (Fig.7a) should be the most sensitive to the soil properties, since it corresponds to the shallowest depth of investigation. In the central part of this map, a band of low resistivity values (roughly $\rho_a \leq 20$ Ohm·m) is observed, extending from the north-western to the south-eastern corner. The boundaries of this zone are almost parallel to the topography.

Within this area the seven plots that seem to be more conductive than others include: 1 (BSF0), 2 (BRF), 4 (BRF0), 11 (MF0), 13 (BRF0), 20 (MF0) and 32 (MF0); It is worth noting that about 85% of these samples are F0 and that there were only three plots in the F treatments that showed slightly more resistivity, namely; 3 (BSF), 12 (MF) and 22 (BSF). Moreover, the highest values of apparent resistivity ($\rho_a > 25$ Ohm·m) were found in the northeast of the central conductive area.Three out of the four southern plots show relatively high resistivity values, around 30 – 35 Ohm·m.

The map corresponding to **a** = 1.0 m (Fig. 7b), the intermediate thicknesses, shows a similar pattern as Fig. 7a. The central conductive strip appears sharper and more homogeneous, especially to the west. The north-eastern resistive area looks also more homogeneous and its southern boundary follows isohypses very well. Compared to the previous map, the southern resistive area is reduced in intensity and dimensions.

The third map (**a** = 2 m) (Fig. 7c), with the greatest depth of investigation, shows a regular gradient from the northeast to the southwest, following the isohypses. The resistivity values decrease from about 40 Ohm·m down to approximately 15 Ohm·m.

It is important to note that as soon as these 3 maps were available, *i.e*. during the survey, 17 points were selected from the entire surface of the BT 1 trial, where auger drillings were performed to establish the relationship between the electrical resistivity distribution and various soil properties, such as its nature, thickness, texture, soil aggregate stability, SW and BD.

These 3 maps definitely allowed us to characterize the spatial variability of the soil properties of the trial. First, these results have assisted in the reclassification of soils of the trial and also formed basis of the further studies. For instance, this this trial was believed to have one soil type known as Vertisol. However, the current study showed there are two soils in this trial which are: Mollic Cambisol to the Northeast and Mollic Nitisol to the South- and Southwest (Mthimkhulu et al., 2016).

4. Discussion

The outcomes of the electrical resistivity mapping of the trial provided four types of information: (i) variation of the soil thickness in relation to topography, which further led to the with two different soil types separated by altitude; ii) Existence of a soil thin layer of colluvium origin, located in the lower part of the trial; iii) Land management influence on soil properties.

i.) Soil thickness

The electrical resistivity (ρ_a) map with the greater depth of investigation (Fig. 7c) shows a high resistivity anomaly in the North-East part, and good correlation with topography. It is enhanced on Fig.8b obtained through low pass filtering of the raw map (a=2m). These results could be due to the closeness of soil surface to the parent rock as a result of shallow depth (<

1 m). The depth of the parent rock was confirmed soil auguring, which additionally led to the reclassification of the soil trial. The soil of the entire trial was initially classified as a Vertisol. For this upper part of trial, it is now re-classified as a Mollic Cambisol (IUSS Working Group WRB, 2014), with a thick well-structured dark AB horizon, directly laying on the weathered dolerite. The deep soil in the South and South Western parts of trial is now classified as a Mollic Nitisol with a dark reddish B horizon (Mthimkhulu et al., 2016). The limit between the two soil types, after Mthimkhulu et al. (2016), is shown on the map (Fig. 8b); it could be better ascertained through additional soundings. It should also be noted that in plots 27 and 28, dolerite stones are visible on the surface, and the thickness of the soil does not exceed 0.5 m.

ii.) Superficial colluvial layer

The electrical resistivity map with (a=0.5 m) the shallowest depth of investigation (Fig. 7a) shows a high resistivity anomaly to the South-West of the trial, which gradually decreases its intensity and extension on the other two maps (Fig. 7b and c) with deeper depths of investigation. It has been proven through augering the soundings and by further physical analysis of the samples that it is due to the presence of a colluvial layer, with higher sand content (Mthimkhulu et al., 2016). Downstream, where the soil has clay loam texture, the sand content is slightly over 20 % only in plots 8 (MF), 16 (BSF0) and 24 (BRF), and this fraction is less than 20% in all other plots. This is also confirmed by the higher BD values on the same plots 8, 16 and 24. The existence of colluvial deposits had never been detected prior to electrical resistivity mapping. It appears to be, as a matter of fact, directly related to the features of the relief.

Land-management effects on electric resistivity

The two maps (SW) and (BD) maps (Fig. 4a and Fig. 5a) showed a clear response to residue treatments: i.e. higher water content and lower bulk density in the M plots, versus lower water content and higher bulk density in the BR plots and intermediate values in the BS plots. From classical scientific literature and our experience, we expected a clear and robust relationship between SW and the electrical resistivity, especially on the map corresponding to the shallowest depth of investigation (Fig. 7a). This anticipation emanated from that SW has a sensitivity to the changes that occur in other soil properties and land management practices. This map, as mentioned above, appears to be strongly influenced by the resistive anomalies related to the thickness of soil and the colluvial layer although, and no obvious consistency appears with the water content at first glance. Thorough analyses of Figure 7a showed that virtually all fertilized plots, except for plot 2, are fully or partially characterized by relatively higher electrical resistivity values compared to the unfertilized treatments. This appears as a major paradox: high electrical resistivity values are observed in the plots with higher water content and, furthermore, these plots have received an additional mineralization.

The relationship between electrical resistivity and soil properties in this trial appears to be more complex than expected. Would that be a general rule in soil sciences?

According to Archie's law,, electrical resistivity of porous consolidated media decreases with increasing SW and mineralisation (Glover et al., 2000). Some results concerning soil studies tend to prove that a somewhat similar law may apply (Michot et al., 2003, McCucheon et al. 2006). According to Cousin et al., (2005) however, the relationship between the electrical resistivity and water content is not so simple, as they showed that electrical resistivity decreases with increase in BD. This may partly of the reasons for the observed high electrical resistivity values in fertilized plots accompanied by a decrease of BD in the current study.

These observations could be due to chemical reactions occurring in the soil.. On the one hand, fertilizers application increases the concentration of ions in the soil which results raises the electrical conductivity of the soil, especially in plots regularly fertilized with potassium chloride (KCl) (Rhoades et al., 1999). On the other hand, changes in the chemical composition and ion concentration of the soil affect its equilibrium and may lead to physicochemical interactions influencing soil aggregation, namely the degradation of soil structural stability.

In a recent publication Paradelo et al. (2013) reported a severe clay dispersion resulting from the application of different forms of KCl and soil acidification (with however no dispersion) where NH^{4+} was applied in a 48 experimental plots located in Versailles. The dispersive effect of K^+ on clays was confirmed by several studies conducted by Marchuk and Rengasamy (2012). In contrast, the study of Van Antwerpen and Meyer (1998) conducted at BT1 trial concluded that K^+ did not cause dispersion due to the release of Al under the low pH conditions. From the same experimental site, Graham et al. (2002) noticed a slight increase in both exchangeable and non-exchangeable K^+ content in the mulched treatment. The major difference recently measured (at BT1) between the different treatments was the significant decrease of divalent exchangeable cations Ca^{++} and Mg^{++} in fertilized plots concomitant with a decrease of pH (Mthimkhulu et al., 2016).

For these last three studies mentioned above, conducted at different years on the BT1 trial, the samples were collected between January and March, which is the time coinciding with the sugarcane growth period. Ion concentrations measured on soil samples collected from the fertilized plots can be relatively higher compared to those in November when electrical resistivity mapping was performed, since nutrients are continuously extracted until the crop is harvested in September or October.

It could also be assumed that fertilizers can be dissolved and leached by rain, since the rainy season begins around August, with a monthly average of 70 mm, reaching its maximum of approximately 120mm in November.

With these observations it could be deduced that the high electrical resistivity values systematically observed in the fertilized plots with chemical inputs (Fig. 6a and b) are due to the soil structural stability degradation, related to complex physicochemical interactions. This deduction is also in agreement with the influence of the so-called pore tortuosity. The tortuosity factor is known to be important in contributing to high resistivity in porous media (Kunetz, 1966). While this factor was well documented for rocks and reconstructed porous media, it is not yet considered for soils and inter-aggregate porosity.

To conclude, we believe that a better understanding of the origin of these high electrical resistivity values in the fertilized plots, requires additional experimental and theoretical work.

The presence of termite nests

The termites of the *Odontotermes sp.* specie are a fungus-culturing termites, making comb nest chambers with large void space that could generate high values of local electric resistivity (Fig. 7a). However, the decrease in the resolution of the measurement with depth make it difficult to separate resistivity features of termite nests from other sources, resulting in high resistivity.

Conclusion

The results of electrical resistivity mapping of the investigated trial showed strong lateral variations associated to the soil thickness, soil texture and other soil properties. The main findings were as follows: i) Soil depth increased from North East to the South West of the trial , but this had no effect the on topsoil characteristics (0-20 cm). This study revealed that the trial was established on two different soils including Cambisol (upper slope) and Nitisol (lower slope) although previous studies have reported a single soil type (Vertisol) in this trial; ii) The increase in soil resistivity and depth in the SW corner of the trial was attributed to accumulation of colluvium material; it may now be considered as a possible hidden limiting factor for sugar cane growth apart from the sole treatment effect, and be included in further investigations of yield variability ; iii). The soil resistivity in the soil surface showed no clear relationship with SW content or bulk density (mulch effect) and this was found to be very strange as SW was significantly higher in the topsoil of M plots; iv). The topsoil resistivity showed some relationship with fertilizer treatments such that higher electrical resistivity observed in fertilized plots was associated with lower soil structural stability measured in the treatment. However the electric resistivity was not related to the inputs of salts (KCl) as fertilizers; v) The termite nests are identified to be more resistant but no correlation with resistant points and termite nests could be established.

The results of the soil electrical resistivity mapping showed that the effect of long term use of fertilizers deeply affects the porous media and soil physical properties, while mulching only temporarily affects the soil surface water content and bulk density, with limited effects on the soil structural and chemical properties at depth.

Geophysical mapping appear as time-consuming and as a relatively heavy operation, but the information it provides makes it largely beneficial, from a methodological, as well as from a practical point of view. However, having reported that, further experimental and theoretical works are still needed to better understand the relationship between electrical resistivity and all classical pedological parameters. The current experimental survey provided an instantaneous pictorial representation of soil variability that was required for the better understanding of the interaction of factors and processes leading to the evolution of this long-term trial.

References

AFNOR NF X31-515., 2005. Mesure de la stabilité d'agrégats de sols pour l'évaluation de la sensibilité à la battance et à l'érosion hydrique, AFNOR, Paris, mars 2005. 13p.

Amezketa, E., 1999. Soil aggregate stability: a review. J. of Sustainable Agric. 14, 83-151.

Bakhsh, A., Colvin, T.S., Jaynes, D.B., Kanwar R.S., Tim U.S., 2000. Using soil attributes and GIS for interpretation of spatial variability in yield. Trans. ASAE 43, 819–828.

Biggar, J. W., Nielsen, D. R., 1976. Spatial Variability of the Leaching Characteristics of a Field Soil. Water Resour. Res. 12, 78-84.

Blair, N., 2000. "Impact of cultivation and sugar-cane green trash management on carbon fractions and aggregate stability for a Chromic Luvisol in Queensland, Australia." Soil & Till. Res. 55, 183-191.

Boix-Fayos, C., Calvo-Cases, A., Imeson, A.C., 2001. Influence of soil properties on the aggregation of some Mediterranean soils and the use of aggregate size and stability as land degradation indicators. Catena. 44, 47-67. DOI: 10.1016/S0341-8162(00)00176-4

Changere, A., and Lal. R., 1997. Slope position and erosional effects on soil properties and corn production on a Mianian soil in central Ohio. J. Sustain. Agric. 11, 5–21.

Corwin, D.L., Lesch, S.M., 2003. Application of soil electrical conductivity to precision agriculture: theory, principles, and guidelines. Agron. J. 95, 455–471.

Corwin, D.L., Lesch, S.M., 2005. Apparent soil electrical conductivity measurements in agriculture. Comput. Electron Agr. 46, 11–43

Cousin, I., Besson, A., Aboubacar Sani, A., Accart, V., Samouëlian, A., Cornu, S., Richard, G., 2005. Influence of soil water content, soil bulk density, soil solution composition on electrical resistivity measurements. EGU 05 Geophys. Res. Abstracts 7, 08150.

Friedman, S.P., 2005. Soil properties influencing apparent electrical conductivity: A review. Comput. Electron. Agric. 46, 45 – 70.

Glover, P.W.J., Hole, P. J., Pous, J., 2000. A modified Archie's law for two conducting phases. Earth Plan. Sci. Let. 180 (3 _ 4), 369 – 383.

Graham, M.H., Haynes, R.J., Van Antwerpen, R., 2002. Size and activity of the soil microbial biomass in the row and interrow of a sugarcane field under burning and green cane harvesting. Proc. S. Afr. Sug. Technol. Assoc. 76, 186-195.

Iqbal, J., Read, J. J., Thomasson, A. J., Jenkins J. N., 2005. Relationships between Soil–Landscape and Dryland Cotton Lint Yield. Soil Sci. Soc. Am. J. 69, 872–882.

IUSS Working Group WRB., 2014. World Reference Base for Soil Resources 2014. International soil classification system for naming soils and creating legends for soil maps. World Soil Resources Reports No. 106. FAO, Rome.

Kemper, W.D., Rosenau, R.C., 1986. Aggregate stability and size distribution. In: A. Klute (Ed.), Methods of Soil Analysis: Part 1, Physical and Mineralogical Methods, 2nd Agronomy Monograph No 9, Book Series 5, Soil Sci. Soc. of Am., Madison, WI, 425–442.

Kravchenko, A.N., Bulloc, D.G., 2002. Spatial variability of soybean quality data as a function of field topography: I. Spatial data analysis. Crop Sci. 42, 804 – 815.

Kunetz, G., 1966. Principles of direct current resistivity processing. Gebruder Borntraeger.

Le Bissonnais, Y., 1996. Aggregate stability and assessment of soil erodibility: I. Theory and methodology. Eur. J. Soil Sci. 47, 425-437.

Li, Y., Lindstrom, M.J., 2001. Evaluating soil quality–soil redistribution relationship on terraces and steep hillslope. Soil Sci. Soc. Am. J. 65, 1500–1508.

Marchuk, A., Rengasamy, P., 2012. Threshold electrolyte concentration and dispersive potential in relation to CROSS in dispersive soils. Soil Res. 50(6), 473-481. http://dx.doi.org/10.1071/SR12135

McCarter, W.J., 1984. The electrical resistivity characteristics of compacted clays.

Géotechnique. 34, 263–267.

McCutcheon, M.C., Farahani, H.J., Stednick, J.D., Buchleiter, G.W., Green, T.R., 2006. Effect of soil water on apparent soil electrical conductivity and texture relationships in a dryland field. Biosyst. Eng. 94, 19–32.

Michot, D., Benderitter, Y., Dorigny, A., Nicoullaud, B., King, D., Tabbagh, A., 2003. Spatial and temporal monitoring of soil water content with an irrigated corn crop cover using electrical resistivity tomography. Water Resour. Res. 39, 11-38.

Milsom J., 2003. Field Geophysics. 3rd Edition, John Wiley & Sons, New York, 244.

Moore, I.D., Burch, G.J., 1986. Physical basis of length-slope factor in the universal soil loss equation. Soil Sci. Soc. Am. J. 50:1294 – 1298.

Mthimkhulu, S., Podwojewski, P., Hughes , J., Titshall , L., Van Antwerpen, R., 2016. The effect of 72 years of sugarcane residues and fertilizer management on soil physico-chemical properties. Agric. Ecosyst. Environ.. 225, 54-61.

Mualem, Y., Friedman, S., 1991. Theoretical prediction of electrical conductivity in saturated and unsaturated soil. Water Resour. Res. 27, 2771–2777. DOI: 10.1029/91WR01095.

Oldenburg, D.W., Li, Y., 1999. Estimating depth of investigation in DC resistivity and IP surveys. Geophysics. 64 (2), 403–416.

Paradelo, R., van Oort, F., Chenu, C., 2013. Water-dispersible clay in bare fallow soils after 80 years of continuous fertilizer addition Geoderma. 200-201, 40-44.

Rhoades, J.D., Manteghi, N.A., Shouse, P.J., Alves, W.J., 1989. Soil electrical conductivity and soil salinity: new formulations and calibrations. Soil Sci. Soc. Am. J. 53, 433–439.

Rhoades, J. D., Chanduvi, F., Lesch, S., 1999. Soil salinity assessment: Methods and interpretation of electrical conductivity measurements. Irrigation and drainage paper, N° 57, 165. FAO, Rome.

Robain, H., Albouy, Y., Dabas, M., Descloitres, M., Camerlynck, Ch., Mechler, P., Tabbagh,

A., 1999. The location of infinite electrodes in pole – pole electrical surveys: consequences for 2D imaging. J Appl. Geophys. 41, 313 – 333.
Robertson, F., 2003. Sugarcane Trash Management: Consequences for Soil Carbon and Nitrogen – Final Report of the Project Nutrient Cycling in Relation to Trash Management. CRC Sugar Technical Publication. CRC for Sustainable Sugar Production, Townsville.
Samouëlian, A., Cousin, I., Tabbagh, A., Bruand, A., Richard, G., 2005. Electrical resistivity survey in soil science: a review. Soil Till. Res. 83, 173-193.
Seaton, W., Burbey, T.J., 2002. Evaluation of two-dimensional resistivity methods in a fractured crystalline-rock terrane. J. Appl Geophys. 51 (1), 21–41.
Senthilkumar, S., Kravchenko, A.N., Robertson, G.P., 2009. Topography influences management system effects on total soil carbon and nitrogen. Soil Sci. Soc. of Am. J. 73, 2059–2067.
Tabbagh, A., Dabas, M., Hesse, A., Panissod C., 2000. Soil resistivity: a non-invasive tool to map soil structure horizonation. Geoderma 97, 393–404.
Thompson, G.D., 1966. The production of trash and its effect as a mulch on the soil and on sugarcane nutrition. Proc. S. Afr. Sug. Technol. Assoc. 40, 333-342.
Van Antwerpen, R., Meyer, J.H., 1998. Soil degradation II: Effects of trash and inorganic fertilizer on soil strength. Proc. S. Afr. Sug. Technol. Assoc. 72, 152-158.
Van Antwerpen, R., Meyer, J.H., Turner, P.E.T., 2001. The effects of cane trash on yield and nutrition from the long-term field trial at Mount Edgecombe. Proc. S. Afr. Sug. Technol. Assoc. 75, 235–241.
Yang, C., Peterson, C.L. Shropshire, G.J., Otawa T., 1998. Spatial variability of field topography and wheat yield in the Palouse region of the Pacific Northwest. Trans. ASAE. 41, 17–27.

Captions and figures

Figure 1a. An aerial view of BT1 trial, with reference to geographical coordinates.

Figure 1b. Schematic view of the experimental site BT 1: 32 plots, 3 types of treatments (BR, BS and M), split between fertilized (F) and unfertilized (F0).

Figure 2. Profile of a Mollic Cambisol located 10 m East of plot 27.

Figure 3. Topographic map and slope gradient vectors: 0.5 m isohypse intervals.

Figure 4a. Map of Soil Water Content (SW), overlaid to topography and to the positions of the collected and analysed samples

Figure 4b. Results of SW measurements with box and whiskers,

Figure 5a. Map of Bulk Density (BD), overlaid to topography.

Figure 5b. Results of BD analysis

Figure 6a. Results of Mean Weight Diameter (MWD), expressed in mm, for the samples collected in the 0 – 10 cm depth range.

Figure 6b. Results of statistical analysis of Mean Weight Diameter (MWD), expressed in mm, for the samples collected in the 10 – 20 cm depth range.

Figure 7a. Electrical apparent resistivity (ρ_a) map, expressed in Ohm·m (Ω·m) for electrode separation **a** = 0.5 m.

Figure 7b. Electrical apparent resistivity (ρ_a) map, expressed in Ohm·m (Ω·m) for electrode separation **a** = 1 m.

Figure 7c. Electrical apparent resistivity (ρ_a) map, expressed in Ohm·m (Ω·m) for electrode separation **a** = 2 m.

Figure 8. Low-pass filtered electrical apparent resistivity (ρ_a) map, expressed in Ohm·m (Ω·m) for electrode separation **a** = 2 m, showing additionally the boundary separating the 2 types of soil to the NE (continuous line) and the limit of the colluvial deposits to the SW (dashed line).

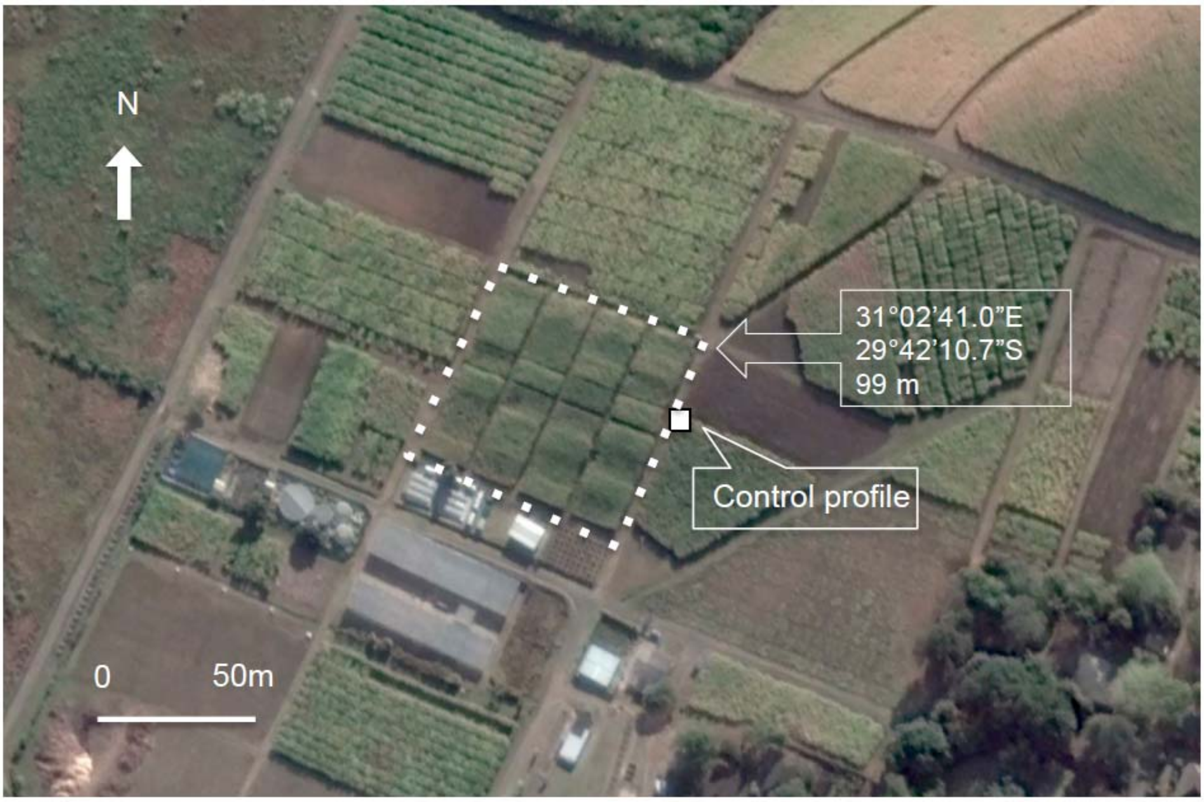

Figure 1a

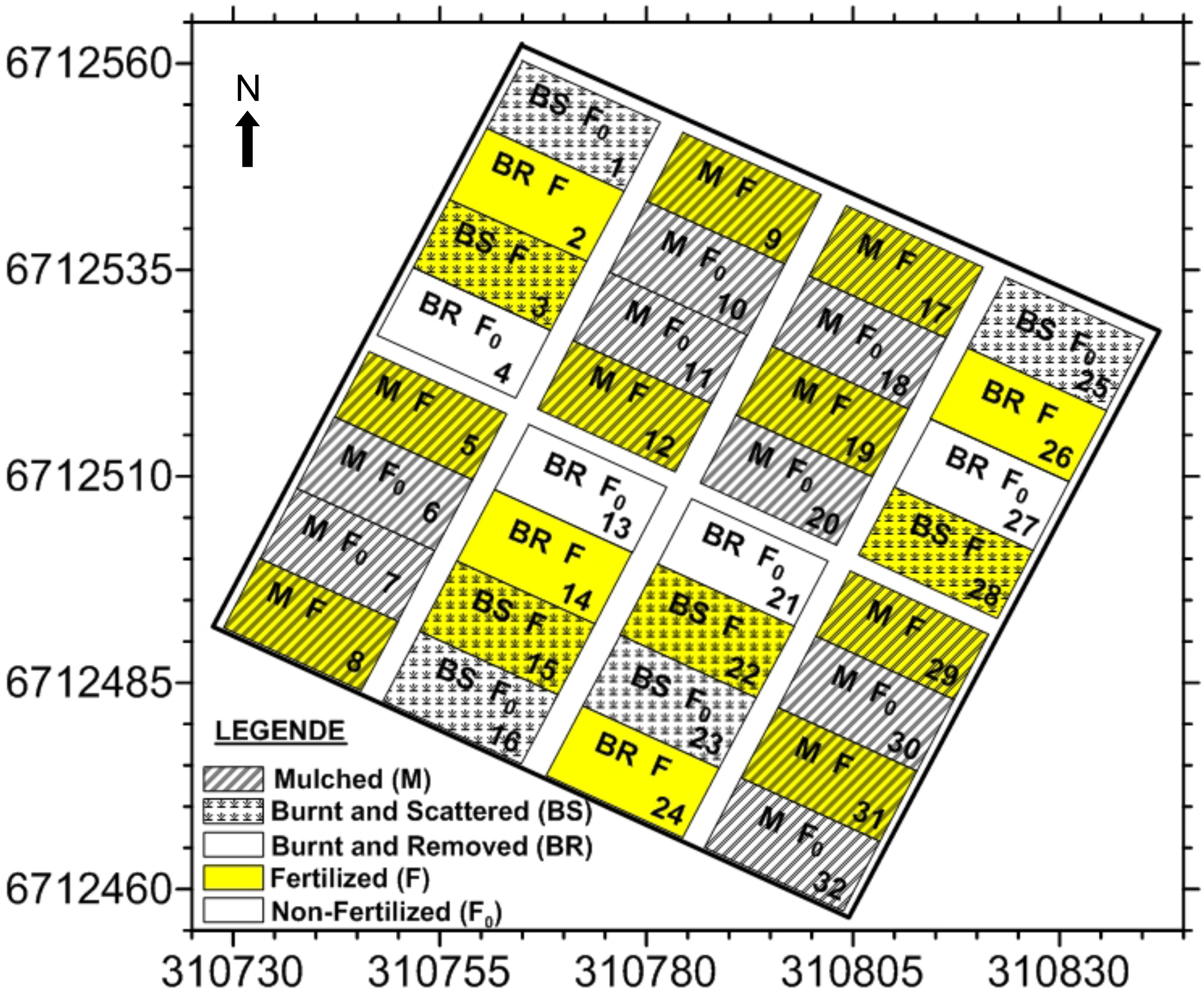
N
6712560
6712535
6712510
6712485
6712460
310730
310755
310780
310805
310830
BS F0 1
BR F 2
BS F 3
BR F0 4
M F 5
M F0 6
M F0 7
M F 8
M F 9
M F0 10
M F0 11
M F 12
BR F0 13
BR F 14
BS F 15
BS F0 16
M F 17
M F0 18
M F 19
M F0 20
BR F0 21
BS F 22
BS F0 23
BR F 24
BS F0 25
BR F 26
BR F0 27
BS F 28
M F 29
M F0 30
M F 31
M F0 32
LEGENDE
Mulched (M)
Burnt and Scattered (BS)
Burnt and Removed (BR)
Fertilized (F)
Non-Fertilized (F0)

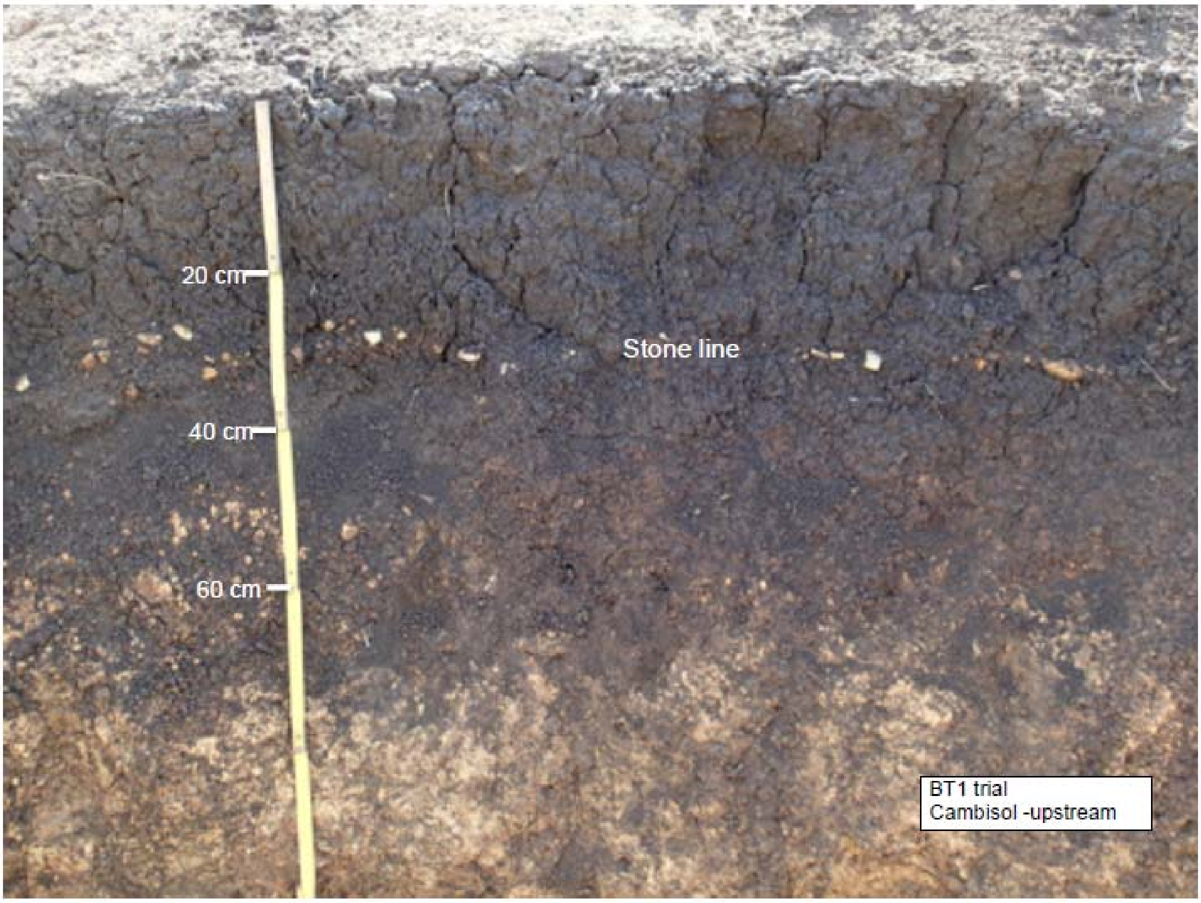

Figure 2

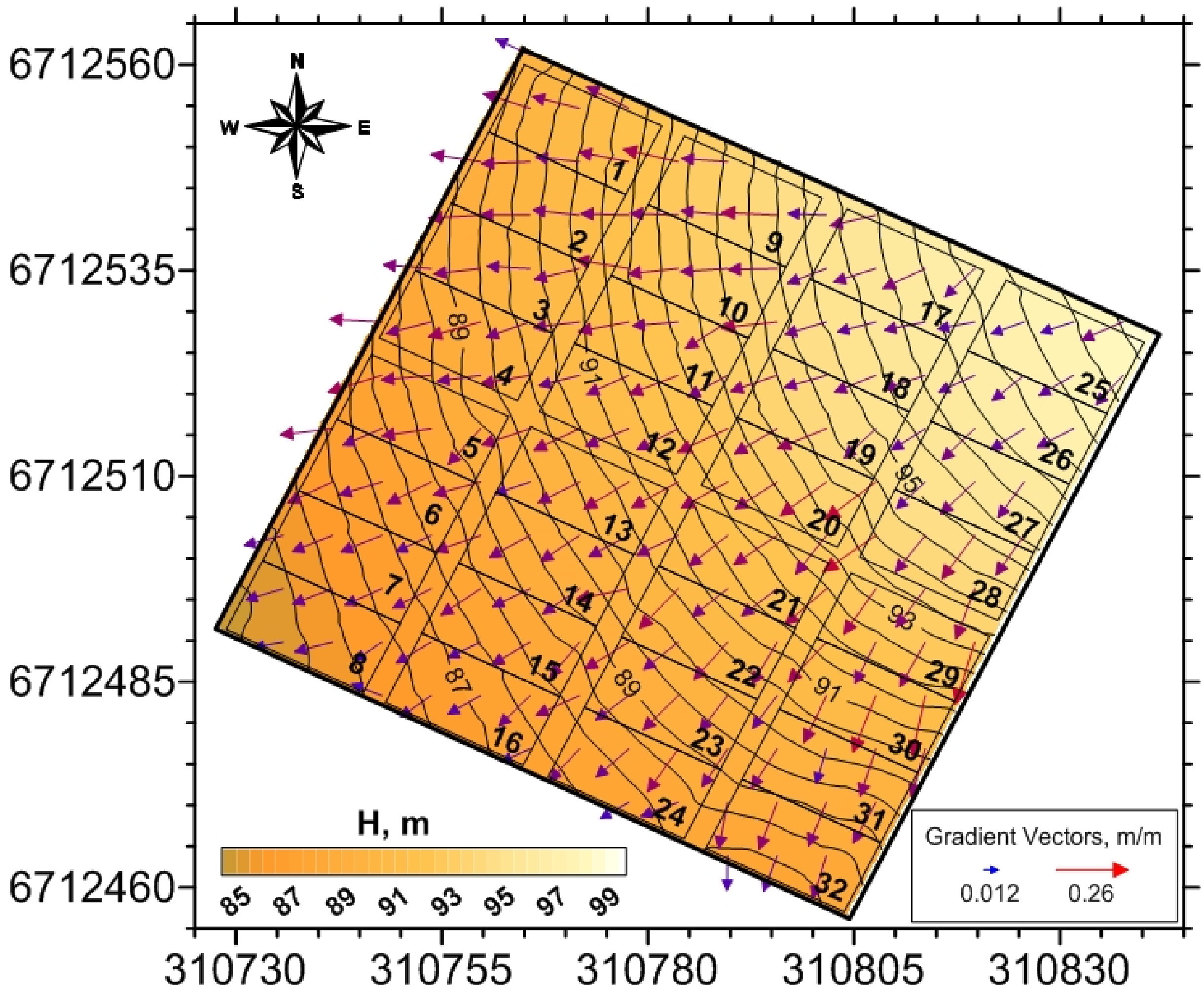

6712560
6712535
6712510
6712485
6712460
310730
310755
310780
310805
310830
N
W
E
S
H, m
85
87
89
91
93
95
97
99
Gradient Vectors, m/m
0.012
0.26

Figure 3

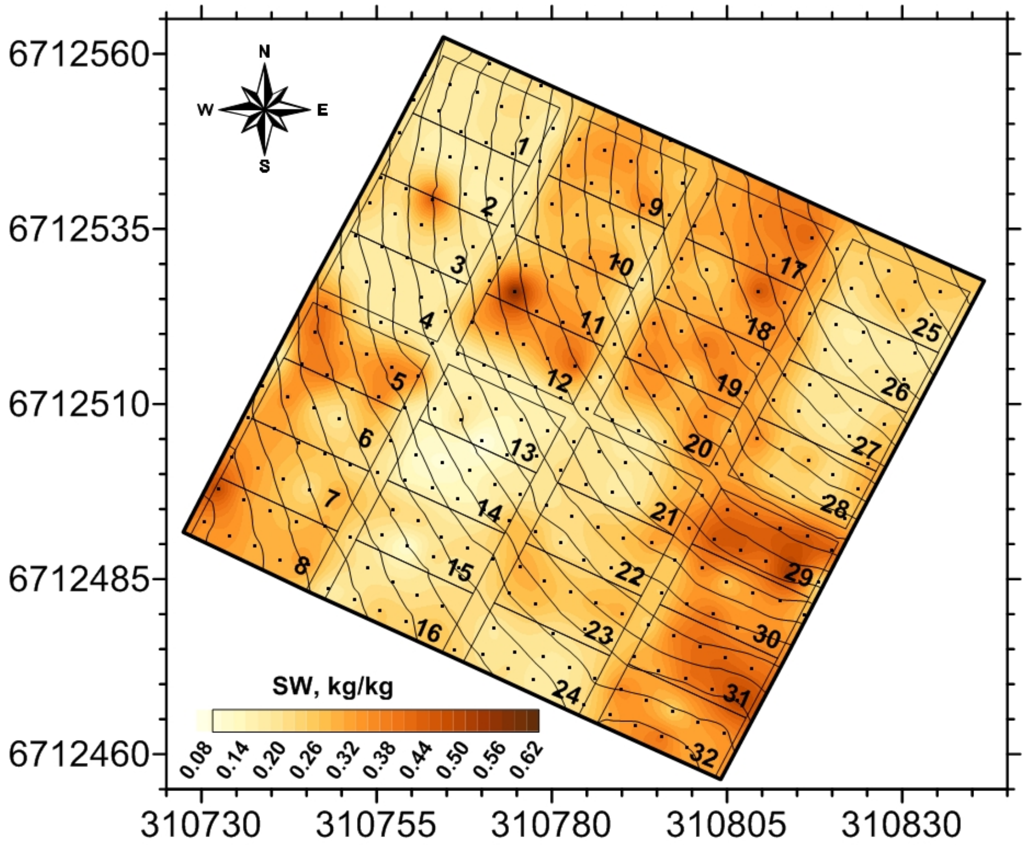
6712560
6712535
6712510
6712485
6712460
310730
310755
310780
310805
310830
N
W
E
S
SW, kg/kg
0.08
0.14
0.20
0.26
0.32
0.38
0.44
0.50
0.56
0.62
1
2
3
4
5
6
7
8
9
10
11
12
13
14
15
16
17
18
19
20
21
22
23
24
25
26
27
28
29
30
31
32

Figure 4a

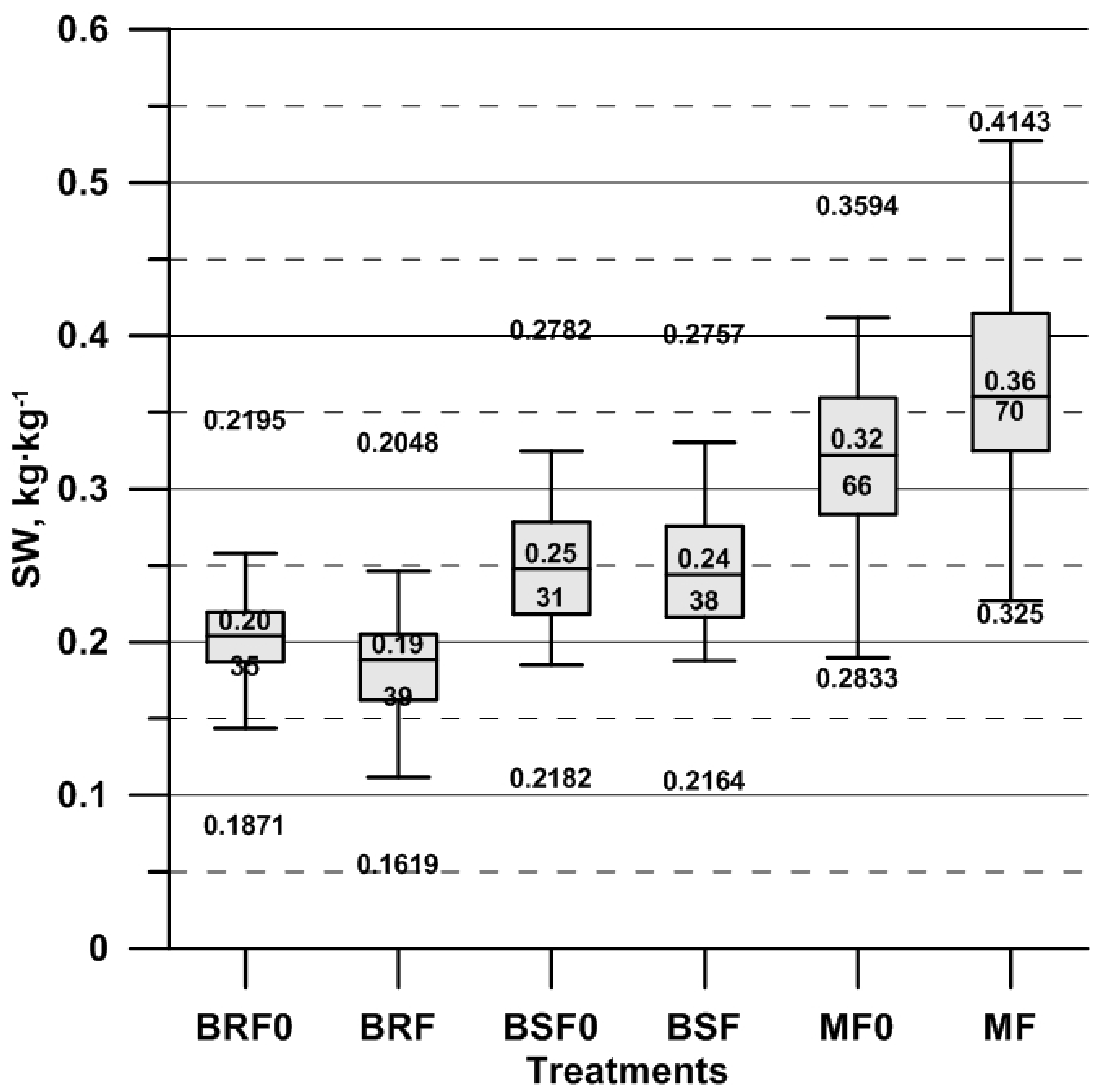

0.6
0.5
0.4
0.3
0.2
0.1
0
SW, kg·kg-1
0.4143
0.3594
0.2782
0.2757
0.2195
0.2048
0.36
70
0.32
66
0.25
31
0.24
38
0.20
35
0.19
39
0.325
0.2833
0.2182
0.2164
0.1871
0.1619
BRF0
BRF
BSF0
BSF
MF0
MF
Treatments

Figure 4b

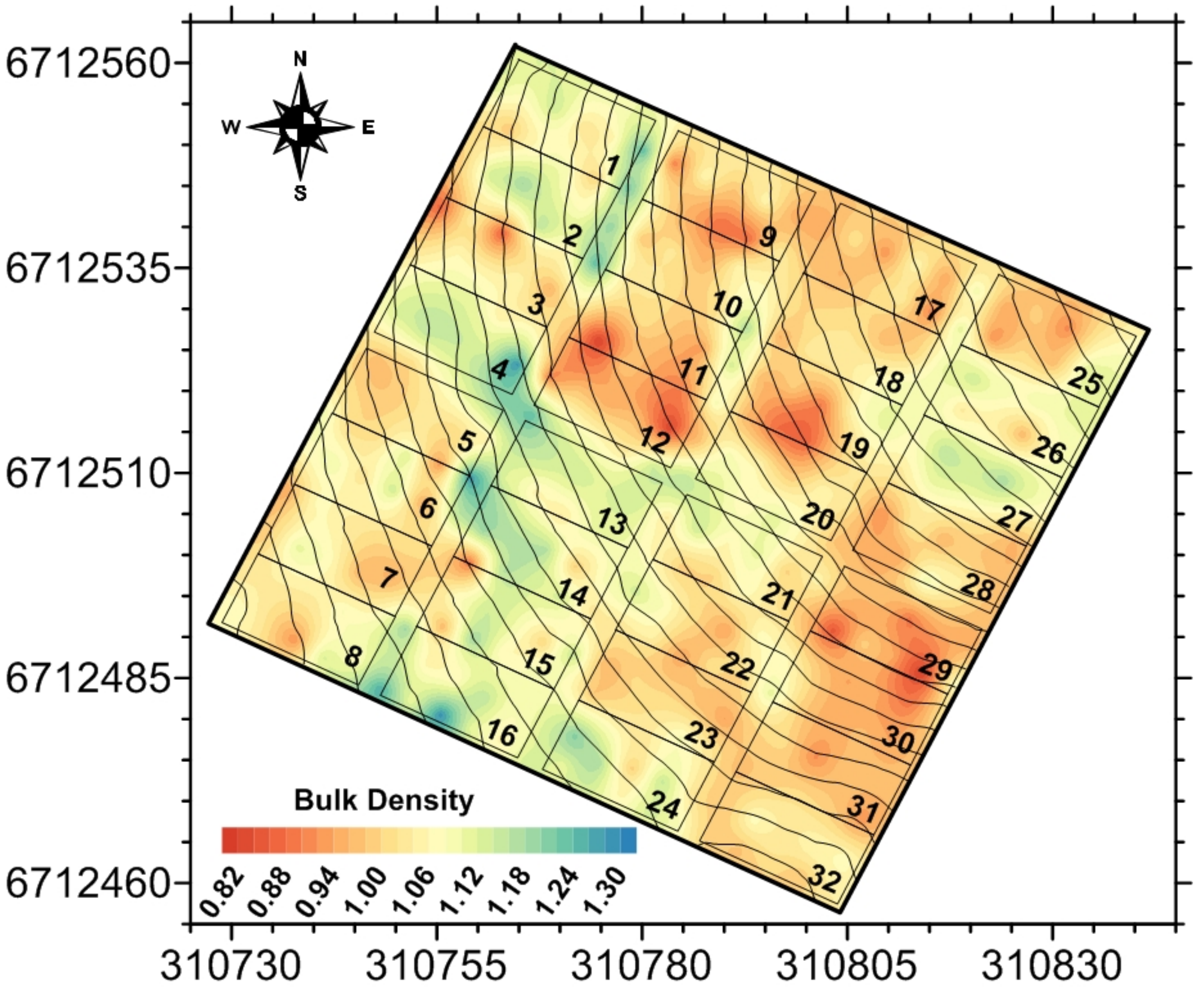

6712560
6712535
6712510
6712485
6712460
310730
310755
310780
310805
310830
N
W
E
S
Bulk Density
0.82
0.88
0.94
1.00
1.06
1.12
1.18
1.24
1.30
1
2
3
4
5
6
7
8
9
10
11
12
13
14
15
16
17
18
19
20
21
22
23
24
25
26
27
28
29
30
31
32

Figure 5a

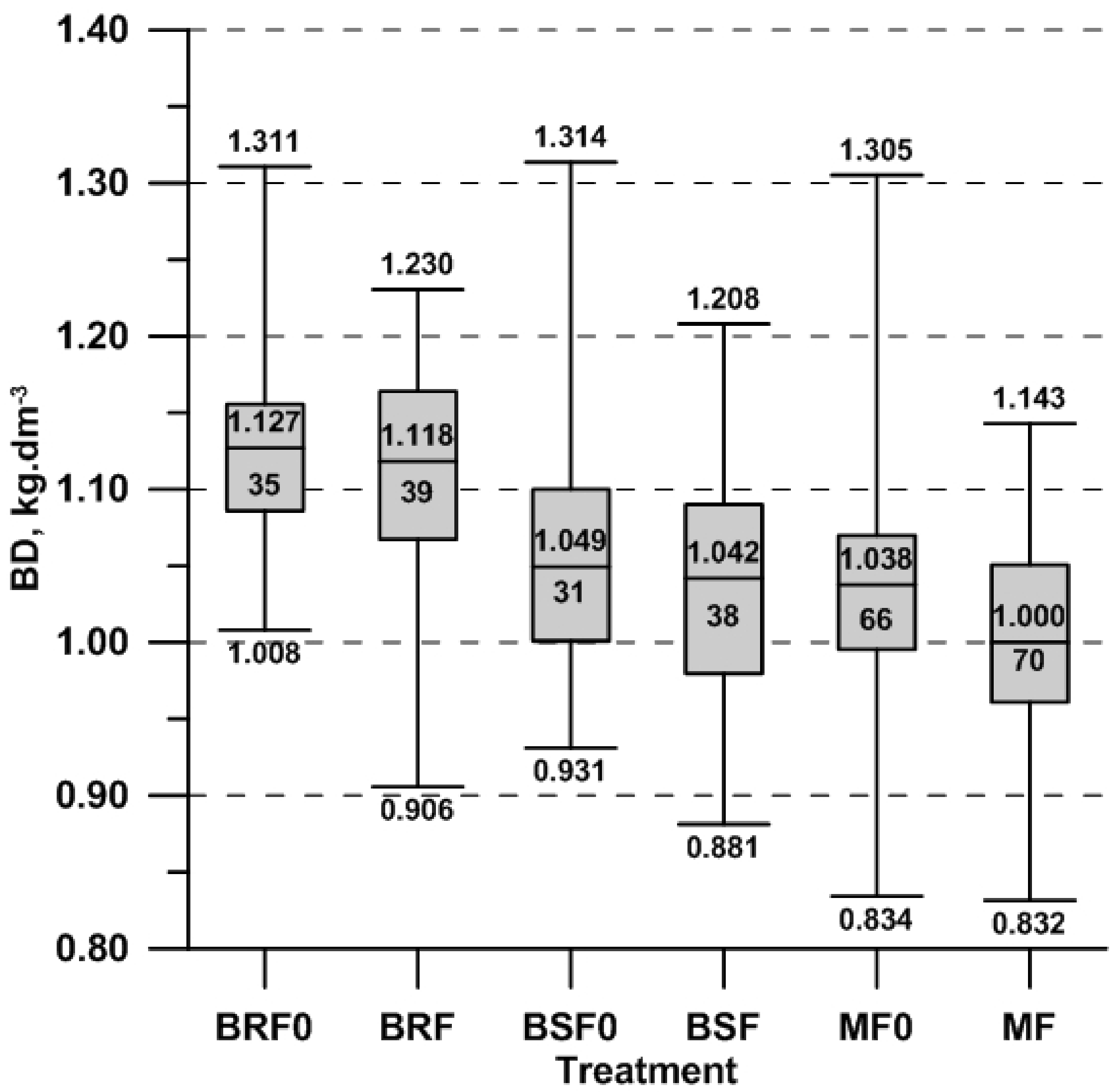
1.40
1.30
1.20
1.10
1.00
0.90
0.80
BD, kg.dm-3
1.311
1.127
35
1.008
1.230
1.118
39
0.906
1.314
1.049
31
0.931
1.208
1.042
38
0.881
1.305
1.038
66
0.834
1.143
1.000
70
0.832
BRF0
BRF
BSF0
BSF
MF0
MF
Treatment

Figure 5b

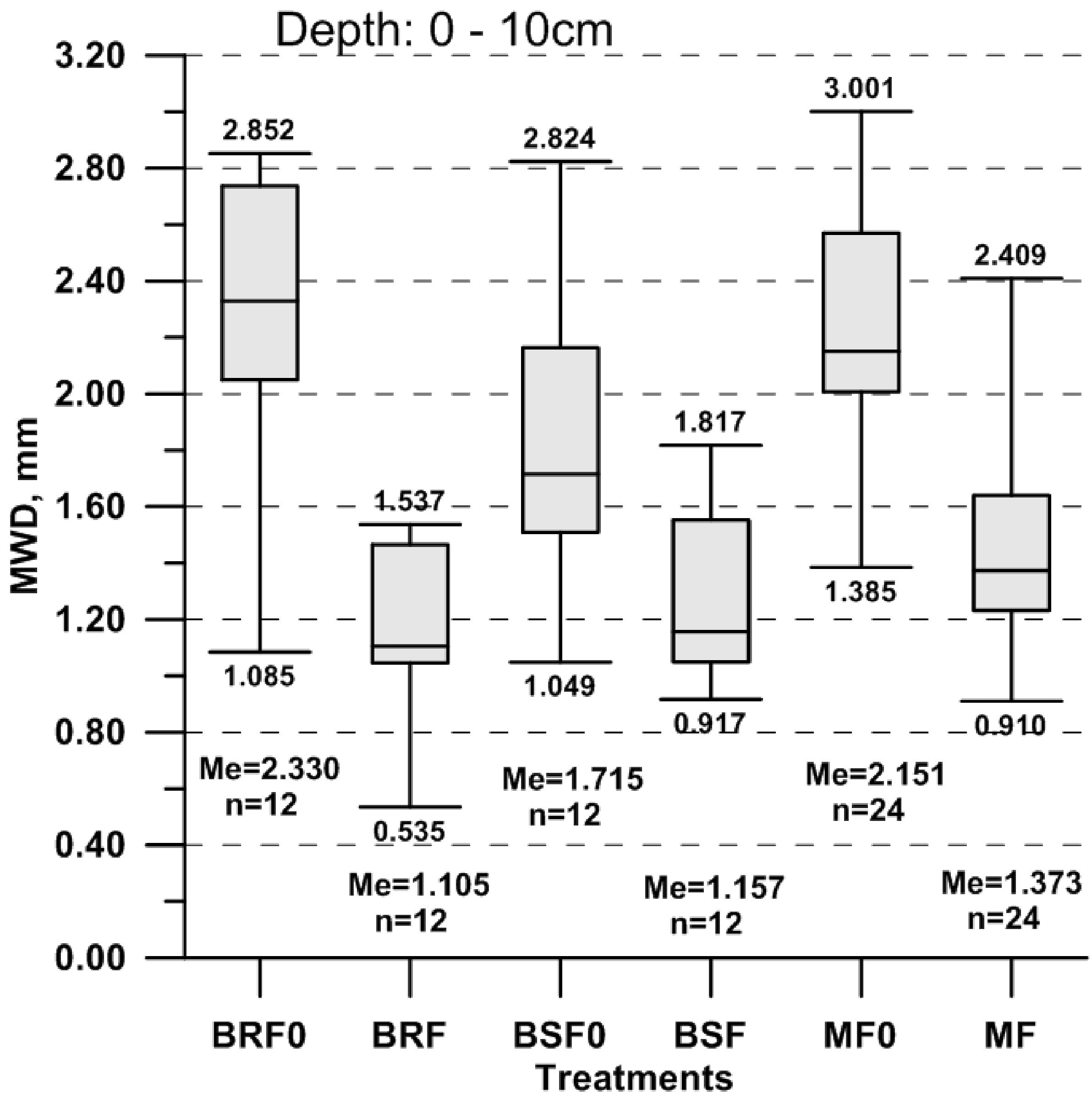

Depth: 0 - 10cm
3.20
2.80
2.40
2.00
1.60
1.20
0.80
0.40
0.00
MWD, mm
2.852
1.085
Me=2.330
n=12
1.537
0.535
Me=1.105
n=12
2.824
1.049
Me=1.715
n=12
1.817
0.917
Me=1.157
n=12
3.001
1.385
Me=2.151
n=24
2.409
0.910
Me=1.373
n=24
BRF0
BRF
BSF0
BSF
MF0
MF
Treatments

Figure 6a

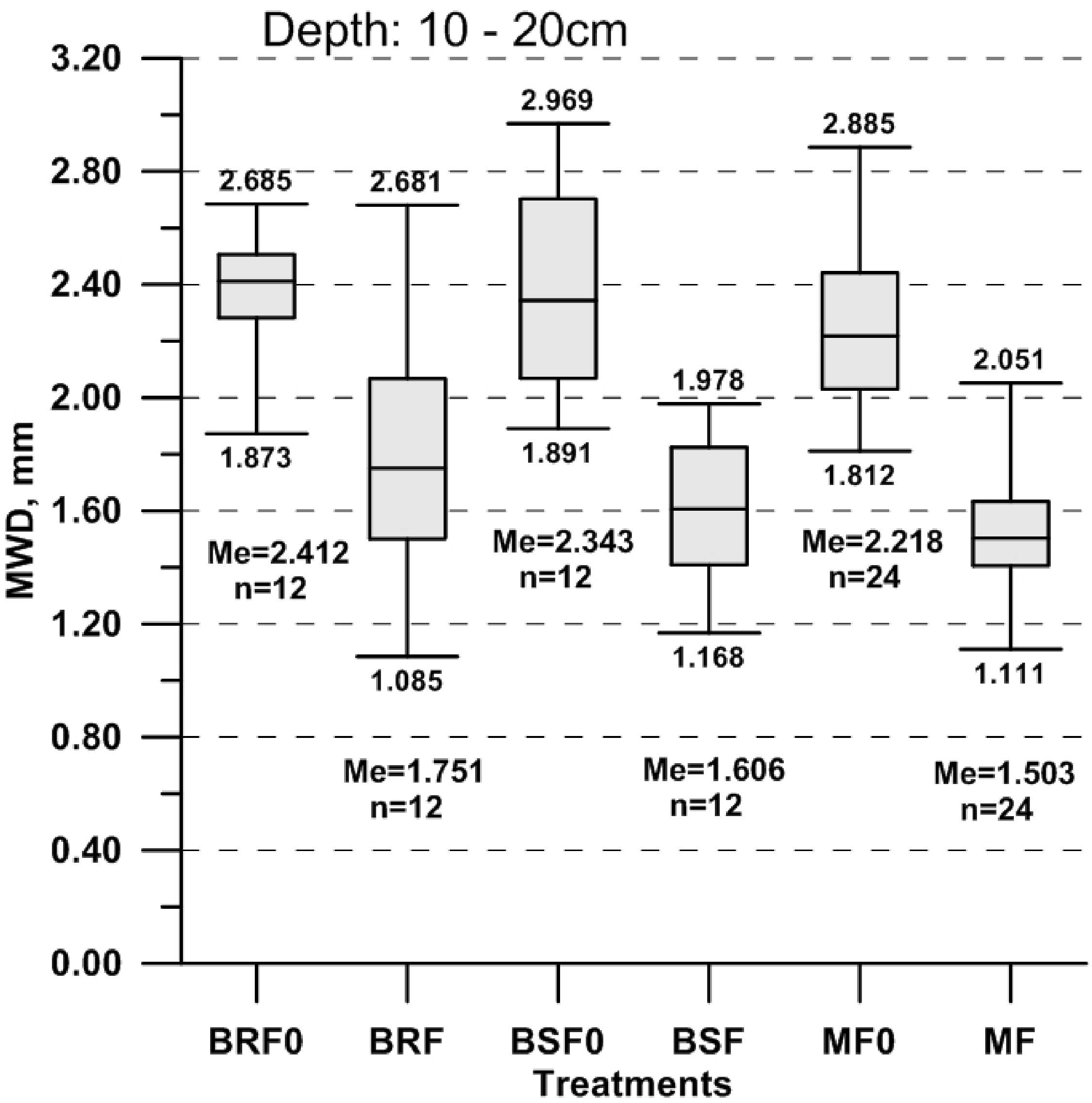

Figure 6b MWD 10 – 20cm

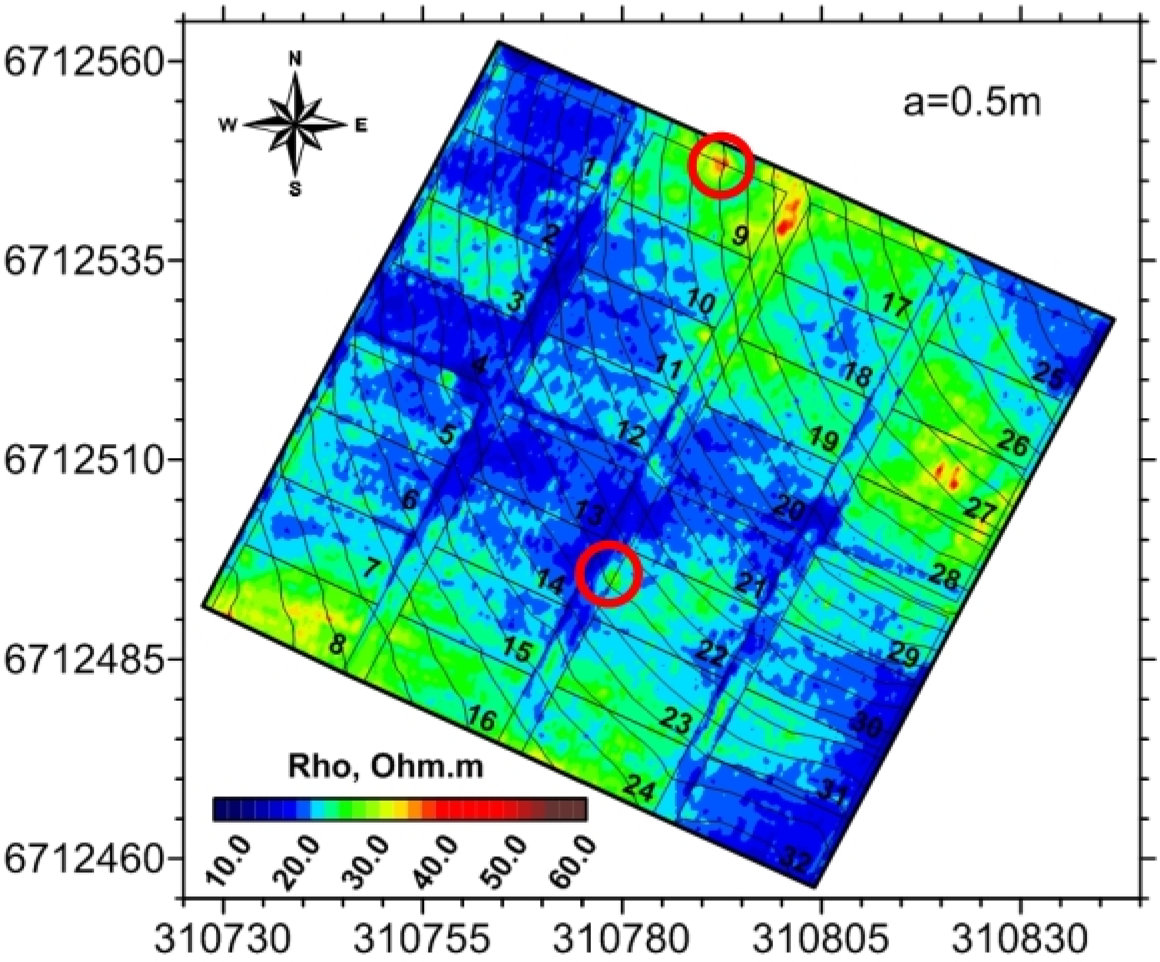
a=0.5m
N
S
W
E
Rho, Ohm.m
10.0
20.0
30.0
40.0
50.0
60.0
6712560
6712535
6712510
6712485
6712460
310730
310755
310780
310805
310830

Figure 7a

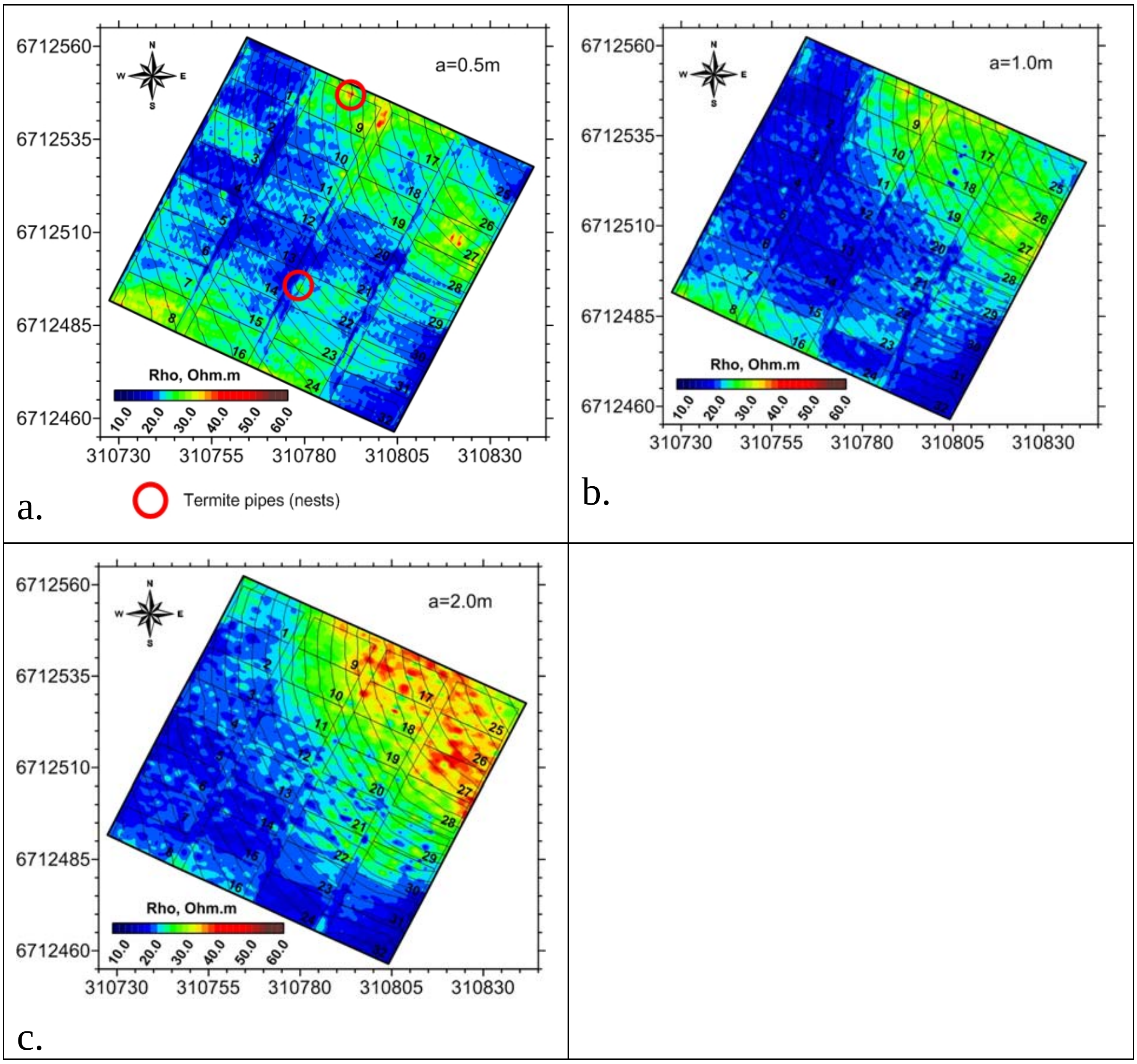

Figure 7a, b and c

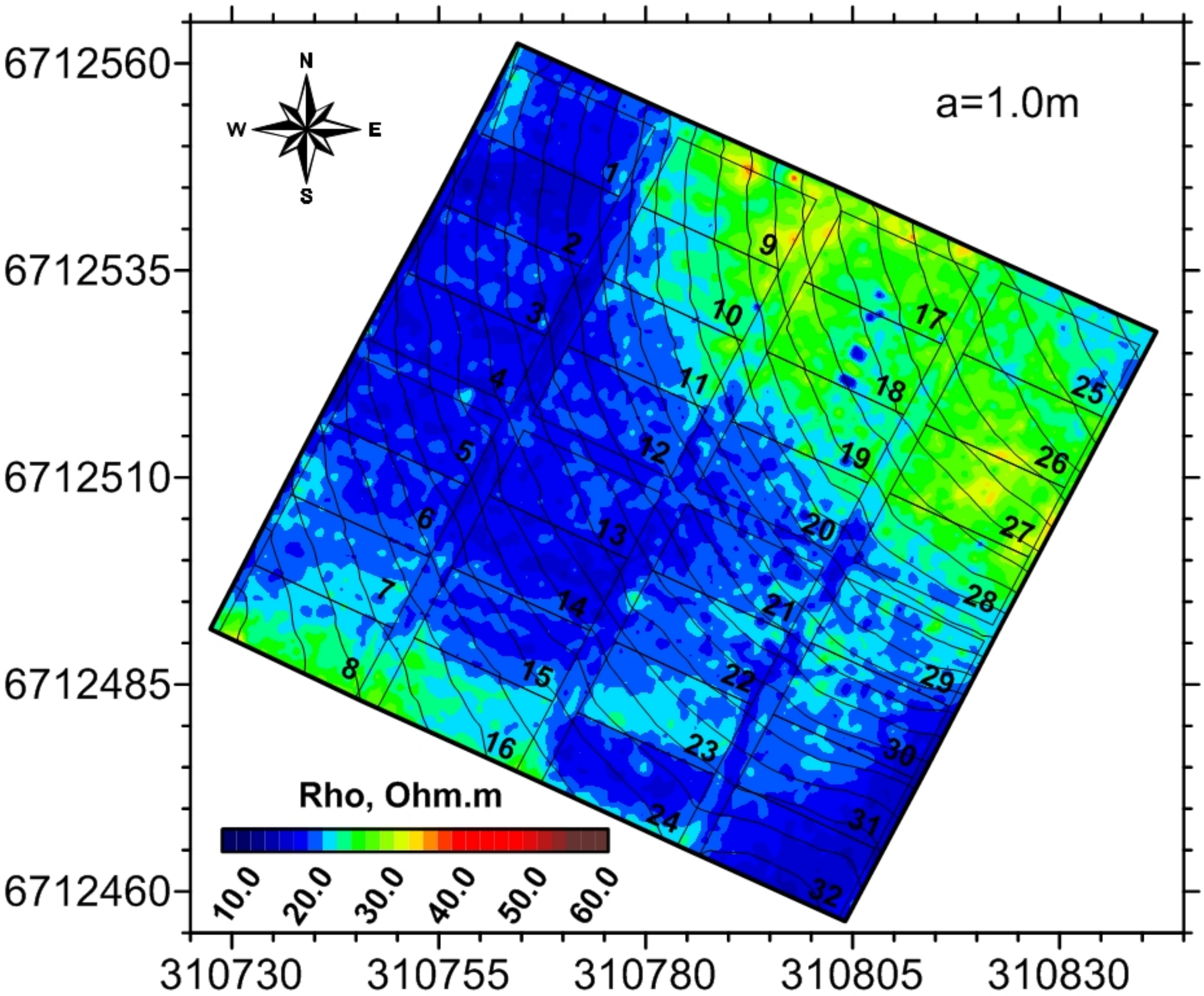

a=1.0m
N
S
W
E
Rho, Ohm.m
10.0
20.0
30.0
40.0
50.0
60.0
6712560
6712535
6712510
6712485
6712460
310730
310755
310780
310805
310830

Figure 7b,

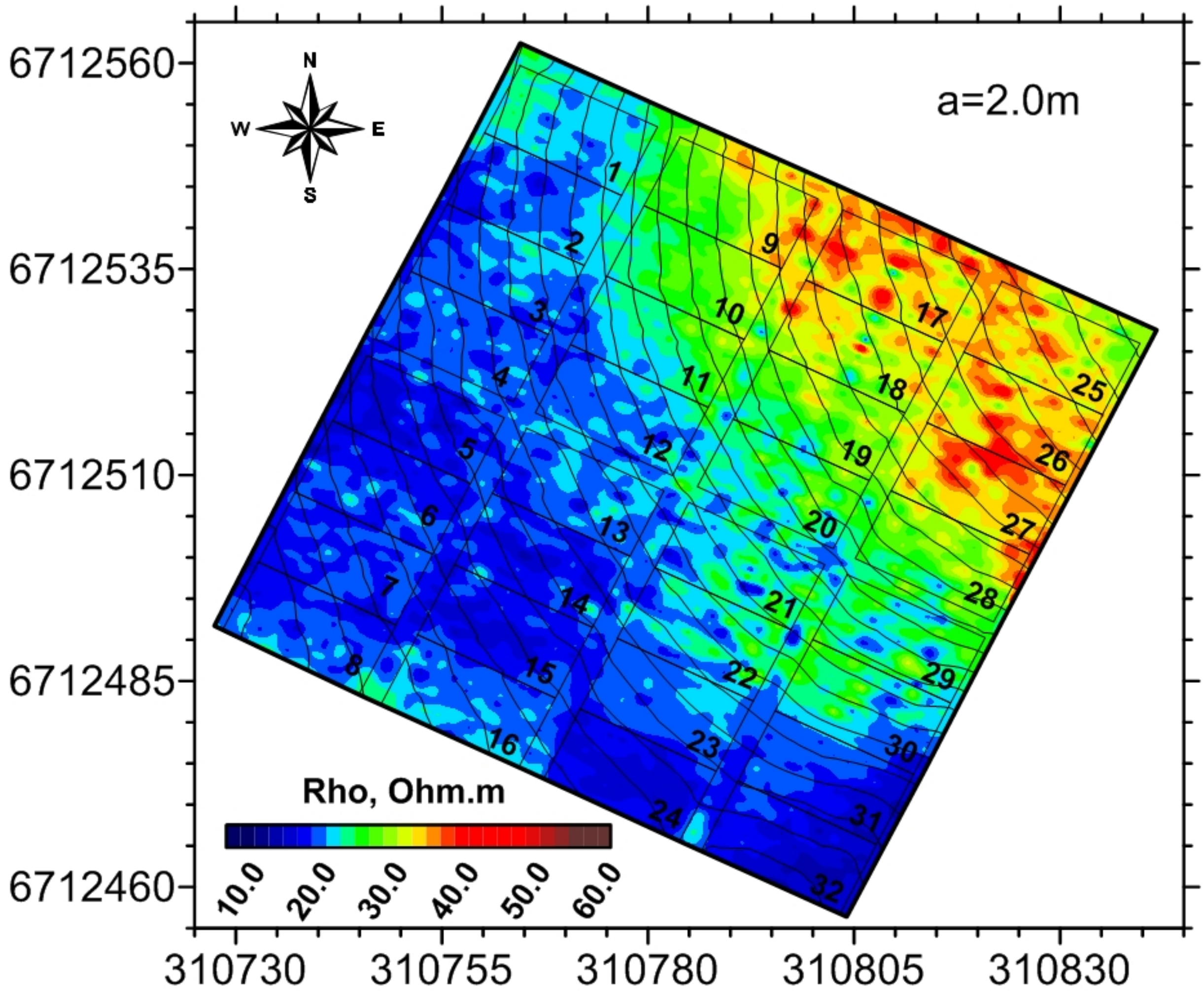

a=2.0m
N
S
W
E
Rho, Ohm.m
10.0
20.0
30.0
40.0
50.0
60.0
6712560
6712535
6712510
6712485
6712460
310730
310755
310780
310805
310830
1
2
3
4
5
6
7
8
9
10
11
12
13
14
15
16
17
18
19
20
21
22
23
24
25
26
27
28
29
30
31
32

Figure 7c

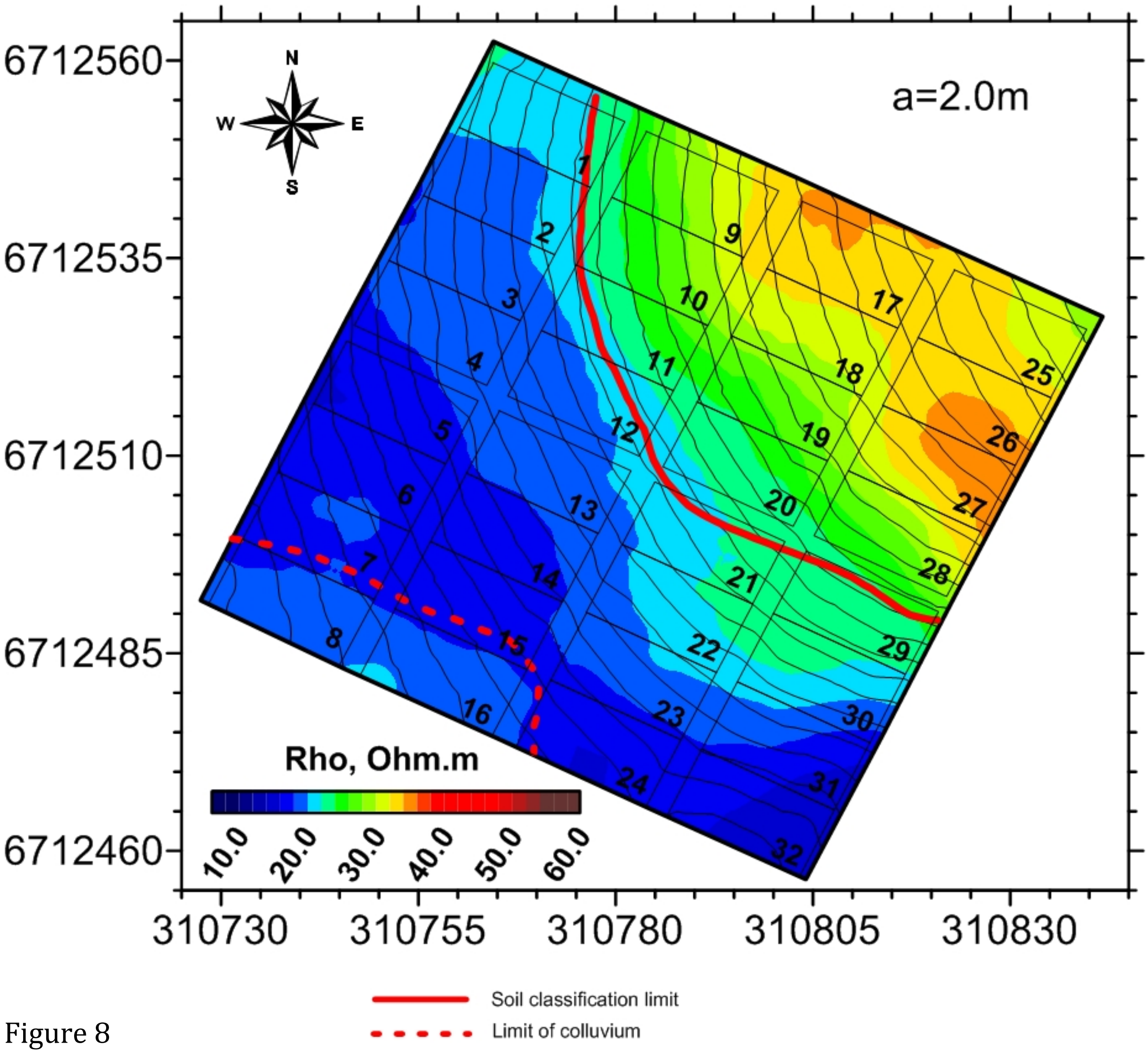
a=2.0m
N
S
W
E
Rho, Ohm.m
10.0
20.0
30.0
40.0
50.0
60.0
6712560
6712535
6712510
6712485
6712460
310730
310755
310780
310805
310830
Soil classification limit
Limit of colluvium

Figure 8